HHS Public Access

Author manuscript

*J Drug Target*. Author manuscript; available in PMC 2015 October 25.

Published in final edited form as:

*J Drug Target*. 2014 August ; 22(7): 648–657. doi:10.3109/1061186X.2014.921924.

# Cellular Uptake and Internalization of Hyaluronan-based Doxorubicin and Cisplatin Conjugates

**Shuang Cai**[1,2], **Adel Ali B Alhowyan**[1], **Qiuhong Yang**[1], **W.C. Melanie Forrest**[2], **Yelizaveta Shnayder**[3], and **M. Laird Forrest**[1,2,*]

[1]Department of Pharmaceutical Chemistry, University of Kansas, Lawrence, KS 66047 USA

[2]HylaPharm, Lawrence, KS 66047 USA

[3]Department of Otolaryngology Head and Neck Surgery, University of Kansas Medical Center, Kansas City, KS 66103, USA

## Abstract

**Background—**Hyaluronan (HA) is a ligand for the CD44 receptor which is crucial to cancer cell proliferation and metastasis. High levels of CD44 expression in many cancers have encouraged the development of HA-based carriers for anti-cancer therapeutics.

**Purpose—**The objective of this study was to determine whether HA conjugation of anticancer drugs impacts CD44-specific HA-drug uptake and disposition by human head and neck cancer cells.

**Methods—**The internalization and cellular disposition of hyaluronan-doxorubicin (HA-DOX), hyaluronan-cisplatin (HA-Pt), and hyaluronan-cyanine7 (HA-Cy7) conjugates were investigated by inhibiting endocytosis pathways, and by inhibiting the CD44–mediated internalization pathways that are known to mediate hyaluronan uptake *in vitro*.

**Results—**Cellular internalization of HA was regulated by CD44 receptors. In mouse xenografts, HA conjugation significantly enhanced tumor cell uptake compared to unconjugated drug.

**Discussion—**The results suggested that the main mechanism of HA-based conjugate uptake may be active transport via CD44 in conjunction with a clathrin–dependent endocytic pathway. Other HA receptors, hyaluronan–mediated motility receptor (RHAMM) and lymphatic vessel endothelial hyaluronan receptor (LYVE-1), did not play a significant role in conjugate uptake.

**Conclusions—**HA conjugation significantly increased CD44 mediated drug uptake and extended the residence time of drugs in tumor cells.

### Keywords

Hyaluronan; doxorubicin; cisplatin; internalization mechanism; CD44 receptors

*Corresponding author at: 2095 Constant Ave., Lawrence, KS, 66047 USA. Tel.: +1 785 864 4388; fax: + 1 785 864 5736. mforrest@ku.edu.

**Disclosures**

SC and AA contributed equally to this work.

**Declaration of Interest**

The remaining authors declare no conflict of interest.

## 1. Introduction

Hyaluronan (HA) is an endogenous glycosaminogly can widely distributed in tissues that cushions joints, forms the eye's humor, give structure to the ECM and plays roles in immunological recognition of infections and inflammation. HA is an anionic glycosaminogly can that is widely distributed throughout the body. It is a biodegradable and biocompatible polymer of 10 to 10,000 kDa that is known to be involved in cell proliferation, migration, and cancer metastasis. Several HA receptors have been identified including CD44, hyaluronan–mediated motility receptor (RHAMM) and lymphatic vessel endothelial hyaluronan receptor (LYVE-1). CD44 is a cell surface adhesion molecule that plays multiple roles in structural and functional interactions between cells. Hyaluronan is the principal ligand for CD44; other CD44-interacting ligands include collagen, fibronectin, and laminin. CD44 binds HA and enables its internalization and intracellular degradation. CD44-HA binding occurs during various physiological events such as cell aggregation, proliferation, and migration, as well as HA endocytosis leading to HA degradation (Fraser et al., 1997).

Our laboratory developed a series of hyaluronan-based chemotherapeutics for locoregional delivery of anticancer drugs, which have demonstrated improved pharmacokinetics, reduced side effects and enhanced *in vivo* antitumor efficacy against multiple cancer xenografts compared to the conventional intravenous therapy of the free drugs (Cai et al., 2008, Cai et al., 2010c, Cohen et al., 2009, Cai et al., 2010b, Cai et al., 2010a, Xie et al., 2010). To understand the boosted bioperformance of the hyaluronan-based drug conjugates and to guide future development of drug-eluting polymeric carriers, we investigated the internalization mechanism and the uptake kinetics of doxorubicin- and cisplatin-releasing hyaluronan conjugates in cancer cells and subsequently in tumor-bearing mice.

In addition to CD44 other receptors that are specifically expressed on certain types of cancer cells may be targeted, so that anti-cancer agents may be internalized more efficiently via receptor-mediated endocytosis. For example folic acid has been incorporated in drug delivery system to target overexpressed folate receptors in cancer cells, including ovarian, lung and breast cancer cells (Zhao et al., 2010, Yue et al., 2013). Zhao et al reported the encapsulation and delivery of doxorubicin using PLGA-PEG-Folate polymeric micelles to target the overexpressed folate receptors on KB cells. Without the carrier, doxorubicin enters cells, both normal and cancerous, nonselectively via passive diffusion; whereas in the presence of a folate conjugated carrier, doxorubicin was preferentially internalized via folate receptor-mediated endocytosis and was liberated from the carrier intracellularly, which resulted in greater cytotoxicity against KB cells. The transferrin receptor is another receptor that is overexpressed on the surface of many cancer cells, such as Non-Hodgkin's lymphoma and melanoma. Transferrin was used as a carrier protein by Singh et al. to attach and deliver doxorubicin chemotherapy. The targeted doxorubicin resulted in greater tumor cell death than free doxorubicin in various cancer cell lines (Singh et al., 1998).

Overexpression of specific receptors in many cancer cells has lead to the development of targeted drug conjugates and carriers that result in improved receptor-mediated

internalization of chemotherapeutic agents in cancer cells compared to conventional chemotherapy. Several monoclonal antibody targeted therapeutics have shown efficacy in the clinical treatment of cancers, such as Herceptin® (trastuzumab), Avastin® (bevacizumab) and Rituxan® (rituximab). Drug conjugates to monoclonal antibodies can both target a receptor involved in tumorgenicity and also deliver a cytotoxic payload to the cancer cells. For example, Seattle Genetics' antibody-drug conjugate brentuximabvedotin delivers the antimitotic agent monomethyl auristatin E to lymphomas using the cancer-associated cell membrane protein CD30, which is a member of the tumor necrosis factor receptor family. The antibody-drug conjugate has been granted accelerated approval from the FDA to be used in patients with Hodgkin's lymphoma and systemic anaplastic large cell lymphoma who have failed prior multi-agent chemotherapy.

## 2. Methods

All chemicals and cell culture supplies were obtained from Fisher Scientific (Pittsburgh, PA) and used as received unless stated otherwise. The internal standard solution and multi-element tuning solution for ICP-MS were purchased from VHG Labs (Manchester, NH). All antibodies were purchased from Ab cam (Cambridge, MA) or Santa Cruz Biotechnology (Santa Cruz, CA) and used as received. Hyaluronan was purchased from Lifecore Biomedical (Chaska, MN). The poly-L-Lysine coated glass coverslips were purchased from BD Biosciences (Franklin Lakes, NJ). The Cy7 N-hydroxysuccinimide (NHS) ester was purchased from Lumiprobe (Hallandale Beach, FL). The Lysotracker blue™ was purchased from Invitrogen. The human oral squamous carcinoma cell line, MDA-1986, was a gift from Dr. Jeffrey Myers (University of Texas, M.D. Anderson Cancer Center; Houston, TX).

### 2.1 Synthesis of Hyaluronan-Doxorubicin Conjugates

The synthesis and characterization of the hyaluronan-doxorubicin (HA-DOX) conjugates were reported previously (Cai et al., 2010a). An adipic acid dihydrazide (ADH) linker was used to facilitate the conjugation of doxorubicin (DOX) to hyaluronan. UV/Vis spectrophotometry at 480 nm was used to determine the degree of conjugation with a doxorubicin calibration curve (1–100 μg/ml). Gel permeation chromatography was also used to confirm the conjugation by equivalent elution times (Gel permeation chromatography; Shodex HQ-806 M column, 0.8 ml/min 20-mM HEPES, pH 7.2) with refractive index and fluorescence detection (ex/em 480/590 nm) (Cai et al., 2010a).

### 2.2 Synthesis of HA-Cy7 Conjugates

The hyaluronan–Cy7 conjugate was synthesized using ADH as a linker. Briefly, HA–ADH (100 mg) was allowed to react with the Cy7 NHS ester (1 mg) at pH 8.3–8.5 overnight in dark. The resulting HA–Cy7 conjugate was dialyzed against 95% ethanol for 24 h (MWCO 10,000 Da), followed by dialysis against 50% ethanol for 24 h (MWCO 10,000 Da). Subsequently, the solution was dialyzed again $ddH_2O$ for 24 h with 3 water changes (MWCO 10,000 Da), followed by freeze-drying. The product was stored at −20 °C freezer until use.

### 2.3 Synthesis of Cy7 labeled HA-DOX Conjugates

The Cy7 labeled HA-DOX conjugate (HA-DOX-Cy7) was synthesized by reacting Cy7 ester NHS with HA-DOX synthesized in section 2.1. The reaction condition was identical to the procedure reported in 2.2. The product was stored at −20 °C until use.

### 2.4 Synthesis of HA-Pt Conjugates

Cisplatin was conjugated to HA (35 kD) based on the previously reported procedure (Cai et al., 2010c, Cai et al., 2010b) with modifications. Typically, HA (100 mg) and cisplatin (40 mg) were dissolved in $ddH_2O$ (20 ml) and stirred in the dark for three days at ambient temperature (ca. 25 °C). The mixture was filtered (0.2-μm nylon membrane) and dialyzed against $ddH_2O$ (MWCO 10,000 Da) for 24 h in the dark. Following dialysis, the crude product was concentrated and stored at ambient temperature in the dark. The degree of cisplatin substitution was determined by inductively coupled plasma mass spectrometry (ICP-MS) for Pt content (Agilent 7500a).

### 2.5 Cell Culture

The head and neck squamous cell cancer cell line MDA-1986 was maintained in Dulbecco's Modified Eagle Medium (DMEM) supplemented with 10% fetal bovine plasma and 1% L-glutamine-alanine.

In the HA-DOX uptake study, prior to imaging, cells were trypsinized and seeded into 12-well plates (100,000–200,000 cells/well) with a polylysine coverslip in each well. Subsequently, cells were co-incubated with sub-microgram per milliliter concentrations of DOX, Cy7, HA-DOX, HA-Cy7, and HA-DOX-Cy7 for 15 m, 1, 6, 24 and 48 h. The cell nuclei and lysosomes were stained using DAPI stain (7.5 μg/ml) and lysotracker blue (150 nM), respectively. For the inhibition experiments, cells were pretreated with the anti-CD44 antibody (10 μg/ml) or chlorpromazine (25 μM) for 30 minutes before the addition of DOX, Cy7, HA-DOX, HA-Cy7, and HA-DOX-Cy7 at both 37 °C and 4 °C. For the HA competition experiments, cells were pretreated with 5- or 10-mg/ml of hyaluronan for 24 h before the addition of DOX, Cy7, HA-DOX, HA-Cy7, and HA-DOX-Cy7. Before imaging, cells were washed three times with phosphate buffered saline (PBS), and the coverslips were fixed on glass microscope slides.

In the HA-Pt uptake study, cells were seeded in 12-well plates (50,000 cells/well). After 24 h, cells were treated with chlorpromazine (25 μM), anti-CD44 antibody (10 μg/ml), anti-RHAMM antibody (10 μg/ml), and anti-LYVE-1 antibody (10 μg/ml) for 1 h before the addition of either cisplatin or HA-Pt. The free cisplatin or HA-Pt conjugate was co-incubated with the cells for 1, 6 and 24 h. Subsequently, cells were washed three times with PBS, trypsinized and collected, and stored at 4 °C until analysis.

### 2.6 Fluorescence Microscopy and Imaging Analysis

The uptake of free drug and conjugates by the MDA-1986 cells was monitored using an inverted fluorescence microscope at pre-determined time intervals. The fluorescence intensities of DOX and the Cy7 bound HA were analyzed and quantified using Image J and the following equation.

Corrected Total Cell Fluorescence (CTCF) = Integrated Density − (Area of Selected Cells × Mean Fluorescence of Background).

Each experiment was performed in triplicate or more. Microscope frames were selected randomly containing typically 20 to 30 cells. Significance between multiple groups was determined by one-way ANOVA analysis with a Tukey Multiple Comparisons post-test and student t-tests (GraphPad Prism 4). A p-value of less than 0.05 was used as an indicator for statistical significance.

### 2.7 Analysis by ICP-MS

The platinum concentrations in either cisplatin or HA-Pt (N=4) treated cells were determined using ICP-MS. The cells were resuspended in 1% $HNO_3$ and sonicated for 1 h before analysis. A platinum calibration curve was generated with a $R^2$ value of greater than 0.99 using concentrations of 50, 100, 200, 500, and 1000 parts per trillion (ppt). Terbium (200 ppt) and bismuth (200 ppt) were used as internal standards.

### 2.8 Platinum Concentrations in Tumor Xenografts

The MDA-1986 human head and neck squamous cell carcinoma cells were prepared in PBS at a concentration of $2 \times 10^7$ cells/ml. Female SCID mice were anesthetized with 2% isoflurane in $O_2$, and 50 μL of cell solution was injected into the oral sub-mucosa of the mice using a 27-ga needle. All procedures in the animal study were approved by the Institutional Animal Care and Use Committee of the University of Kansas.

This xenograft model has been used in our laboratory to evaluate a hyaluronan-based drug delivery system (Cai et al., 2010b). Typically, the primary tumors with sizes between 5 to 150 $mm^3$ were observed on the cheeks within 2 weeks after cell implantation. The tumor growth was monitored twice weekly by measurement with a digital caliper in two perpendicular dimensions, and the tumor volume was calculated using the equation: tumor volume = $0.52 \times (\text{width})^2 \times (\text{length})$.

Animals bearing head and neck tumors were randomly divided into 2 groups, including the subcutaneous HA-Pt group (N=4/timepoint) and the intravenous cisplatin group (N=4/timepoint). When the tumor reaches 100 $mm^3$ in size, HA-Pt was administered subcutaneously next to the tumor at a dose of 5 mg/kg on the basis of platinum. Cisplatin (3 mg/ml) was injected intravenously via the tail vein. The animals were euthanized at 2, 24 and 48 hours post injection. The tumors were excised and stored at −80 °C until analysis.

To determine the platinum concentrations in tumors, approximately 30 mg of tumor tissues excised at each timepoint were homogenized in 10% $HNO_3$ using a Tissue Tearor homogenizer (Cole-Parmer, Vernon Hills, IL), heated at 80 °C for 4 hours, and centrifuged at 1,000× g for 10 minutes. Subsequently, the supernatant of the tissue homogenate was diluted by 300–500 fold using 1% $HNO_3$ and vortexed vigorously before ICP-MS analysis.

# 3. Results

## 3.1 Synthesis of Hyaluronan-based Conjugates

The synthesis and characterization of the HA-Pt and the HA-DOX conjugates was reported in our previous studies (Cai et al., 2010b, Cai et al., 2010a). The drug loading degrees of the HA-Pt and the HA-DOX conjugates were calculated to be approximately 20%wt and 3%wt, respectively (Xie et al., 2010, Cai et al., 2010a). The addition of the Cy7 fluorophore on the polymer backbone allowed the internalization and the cellular distribution of the conjugates to be visualized using fluorescent microscopy. The degree of Cy7 labeling (<1%, data not shown) was minimized to avoid any substantial modifications of the intrinsic characteristics of the polymer and drug conjugate.

## 3.2 Fluorescence Imaging of HA-DOX Conjugate in Cells

The fluorescence spectroscopy of doxorubicin and Cy7 was collected using a fluorophotometer. The Cy7 and DOX have minimum spectrum overlap. The peak fluorescence spectra were: DOX, 480 nm (ex) and 560 nm (em); Cy7, 750 (ex) and 773 nm (em) (Figure 1).

The cellular uptake of DOX, HA-DOX, HA-Cy7, and HA-DOX-Cy7 was monitored at 15 min, 1, 6, 24 and 48 h after the addition of each treatment. The timepoints were selected so that the cellular trafficking of the drug and the carrier may be investigated during cells' entire life cycle (the cell division time of MDA-1986 cells is 20–24 h). The free doxorubicin entered cells within 15 min and mainly localized in the cell nucleus for 48 h (Figure 2). The Cy7 labeled HA was internalized and remained in the cytosol from 15 min to 48 h (Figure 3). Interestingly, the HA-DOX conjugates were found to be localized in two cellular compartments – the nucleus and the cytosol, which were attributed to the presence of both unbound doxorubicin that had been released from the carriers and entered the nucleus, and bound drug that remained in the cytosol and acted as a drug-releasing depot (Figure 4). To verify the doxorubicin localization in the nucleus, cells were stained with 7.5-μg/ml DAPI for 5 minutes before imaging (Figure 2F and 4F).

To evaluate the co-localization of doxorubicin and the nanocarrier simultaneously, the cells were treated with Cy7 labeled HA-DOX conjugates at 15 min, 1, 6, 24 and 48 h (Figure 5). At 15 min, the cellular fluorescence signals were relatively low in both the doxorubicin and the Cy7 channels; whereas starting from 1 h the localization of doxorubicin in the cell nucleus and the distribution of the fluorescent carriers in the cytosol became evident. At 48 h, a substantial amount of conjugates was widely distributed in the cytoplasm where doxorubicin was still bound to HA as indicated by the yellow color in either the cytosol or especially near the nuclear membrane.

The cellular internalization pattern of HA-DOX differed from either free DOX or unconjugated fluorescent HA (HA-Cy7). Specifically, 15-minute incubation of HA-DOX in MDA-1986 cells resulted in limited increase of DOX fluorescence intensity in the cytosol. After 1 h co-incubation, two patterns of DOX distribution occurred in cell populations, one of which exhibited increased fluorescence in cytosol compared to the 15-min experiment. Another population of cells started to show elevated nuclear DOX fluorescence, suggesting

the *in vitro* release of the free DOX, followed by nuclear entry. From 6 to 48 h post-treatment, the intensity of the nuclear DOX fluorescence continued to increase until it reached its maximum at 48 h, indicating the continuous cellular uptake of the HA-DOX conjugate and the sustained release of the active drug. Furthermore, the HA-DOX-Cy7 conjugate demonstrated a similar kinetic pattern as the HA-DOX conjugate, both of which suggested that the conjugate released doxorubicin in the cell in a sustained-release fashion for an extended period of time.

Additionally, the highest fluorescence intensities in doxorubicin- and HA-DOX-treated cells were determined to be 6 and 24 h, respectively. The prolonged $T_{max}$ in the HA-DOX experiment elucidated that the carrier serviced as a doxorubicin-eluting depot *in vitro*, which is consistent with our previous finding using breast cancer xenografts, in which tumor-bearing mice were injected peritumorally with HA-DOX. After 1 day, 10% of the initial HA-DOX was found in the area of the tumor and 66% was found in the area of the tumor-draining lymphatics and local tissues. After a week, 4% of the original dose still remained in the primary tumor with 10% of the initial dose in the surrounding area and adjacent lymph nodes (Cai et al., 2010a).

The maximum fluorescence intensities of HA-Cy7- and HA-DOX-Cy7-treated cells were determined to be 24 and 6 h, respectively. The free Cy7 was used as a control, and it entered cells and reached its maximum signal in an hour (data not shown). The $T_{max}$ of the HA-DOX-Cy7 uptake was found to be shorter than that obtained from the HA-Cy7 experiment, possibly due to the early release of the doxorubicin.

The lysosomes are known to play a role in the degradation of nanoparticles and drug conjugates *in vitro* (Lunov et al., 2010, Malugin et al., 2007). The MDA–1986 cells were incubated with lysotracker blue, an organelle–specific dye for staining the lysosomes, in the presence of different conjugates for 1 h before imaging. The lysotracker dye was found to be co-localized with the fluorescence generated by doxorubicin, suggesting that lysosomal environment is likely to act as a sequestering compartment for doxorubicin (Figure 6) (Sakai-Kato et al., 2012), which is consistent with the behavior of small molecule weak bases (Duvvuri et al., 2004).

### 3.3 Uptake Mechanism of HA-DOX Conjugate in Cells

Because nanoparticles and conjugates have been known to use the endocytic pathway to enter cells, we speculated that the inhibition of this pathway may result in reduced degree of internalization of the carriers and the conjugates. Our assumption was tested by pretreating cells using 25–μM chlorpromazine for 30 min before the addition of the HA conjugates. Chlorpromazine is a cationic amphipathic drug that inhibits endocytosis via a clathrin–mediated pathway. Subsequently, the cells were imaged and analyzed semi-quantitatively using the Image J. The results were reported in Figure 7. The chlorpromazine–treated cells exhibited 69% less fluorescence signal of the HA–Cy7 compared to the nontreated cells ($p=0.0033$), suggesting that the exposure to chlorpromazine resulted in decreased internalization of the HA conjugate, possibly due to the hindered endocytosis (Figure 7). Similar observations were made from the HA–DOX and the free DOX experiments, where the chlorpromazine–treated cells demonstrated a 29% ($p=0.0003$) and a 28% ($p=0.0018$)

reduction in the relative fluorescence intensity in relation to the nontreated groups, respectively (Figure 7).

Anti–CD44 antibodies bind to CD44, the primary receptor for hyaluronan, and inhibit the receptor–mediated endocytosis of HA. In the HA–Cy7 and the HA–DOX treatment groups, anti-CD44 antibody pretreated cells demonstrated a 33% ($p=0.0047$) and a 23% ($p=0.0023$) reduction in the relative fluorescence intensity compared to the non-treated cells, respectively (Figure 7 and 8). As a control, in the DOX groups, both non-treated and anti-CD44 treated cells had similar relative fluorescence signals (Figure 7). The result indicated that the CD44 pathway may act as a major uptake route for the internalization of the HA conjugates.

Receptor–mediated endocytosis is a saturable process, in which the uptake of the molecules will be hindered if all the receptors have been occupied. By exposing cells to an excess of HA prior to the addition of the HA conjugates, a reduction in the degree of conjugate uptake is likely to occur if both unmodified HA and HA conjugates utilize the same receptor to gain access to cells. It was found that pretreatment of cells with 5– or 10–mg/ml HA for 24 h prior to the addition of the Cy7 labeled HA resulted in a 29% ($p=0.0325$) and a 53% ($p=0.0011$) reduction in the relative fluorescence intensity compared to the non-treated cells, respectively (Figure 7). Further, a 10–mg/ml HA pretreatment caused a 14% ($p=0.0276$) reduction in the relative fluorescence intensity in cells treated with HA–DOX compared to the non-treated cells (Figure 7). The internalization of free doxorubicin remained unaffected by the exposure to either the 5– or the 10–mg/ml HA.

It is expected that the uptake of HA-DOX conjugates would be inhibited by chlorpromazine; however it is interesting that the internalization of the free doxorubicin was also affected in the presence of an endocytosis inhibitor. Many small molecules (MW <500 g/mol) enter cells via passive diffusion. However, evidences of transporter–mediated uptake of doxorubicin and daunorubicin have been reported (Majumdar et al., 2009). Furthermore, the anti-CD44 antibody blocking study suggested that the internalization of both the HA-DOX and HA-Cy7 conjugates were greatly impacted by blocking CD44, the primary receptor of hyaluronan. It indicated that the CD44 pathway may act as a major uptake route for the internalization of the HA conjugates.

Cellular uptake via receptor-mediated endocytosis is an energy-dependent process. Incubation of cells at 4 °C disturbed the normal uptake patterns of both the drug and the conjugates by lowering the degree of molecule internalization. The cellular HA-DOX and DOX fluorescence intensities were reduced by 81% and 86% at 4 °C compared to their counterparts at 37 °C (Figure 8), further supporting the previous finding that the internalization of the HA conjugates is likely to be governed by energy-dependent mechanisms including an endocytotic process.

### 3.4 Uptake Mechanism of HA-Pt Conjugate in Cells

The cellular platinum concentrations were determined quantitatively using ICP-MS in cells treated with chlorpromazine, anti-CD44, anti-RHAMM, or anti-LYVE-1 antibodies prior to the addition of the HA-Pt or the cisplatin control. The durations of the exposure to the HA-

Pt or cisplatin in cells were 1, 6 and 24 h, to capture both the earlier and the later kinetics of platinum internalization. The release half-life of the platinum-releasing conjugate was calculated to be approximately 10 h in our previous study, thus, within 24 h a significant percentage of the platinum may have been liberated from the carrier HA. The platinum concentrations in the anti-CD44 antibody treated cells was 49% lower than that in the non-treated cells ($p=0.0154$) at 6 h (Figure 9), whereas the platinum concentrations in either the anti-RHAMM or the anti-LYVE-1 treated cells were statistically similar to that in the non-treated cells at 6 h, indicating that the HA-Pt conjugate is likely to be internalized via CD44-mediated endocytosis. At 1 h, the platinum concentrations in all HA-Pt treatment groups were similar and were approximately 30% of the platinum concentrations of the 6-h experiments. Further, at 24 h, the majority of the platinum has been released from the HA and cellular platinum concentrations are similar within all treatment groups.

Besides CD44, other HA-relevant cellular receptors, including RHAMM/CD168 and LYVE-1, have been reported to be involved in the interaction and internalization of hyaluronan (Hall et al., 2001, Johnson et al., 2007). RHAMMMs are expressed on the cell surface, interacting with HA and regulating the migration and proliferation of cells after they interact with HA. Studies have been reported that the RHAMMs are expressed in many cancer cells, including head and neck squamous cell cancer cells (Yamano et al., 2008, Shigeishi et al., 2009). LYVE-1s are known as surface receptors of the lymphatic vessel endothelial cells, playing a role in the transport of both soluble and immobilized extracellular matrix mucopolysaccharidehyaluronan. However, the expression of LYVE-1 gene is not restricted to the lymphatic vessel endothelial cells; cancer cells including liver cancer cells (Mouta Carreira et al., 2001) and non-small cell lung cancer cells (Chang et al., 2011) also express LYVE-1. To elucidate the roles of CD44, RHAMM and LYVE-1, and to understand their impacts on the internalization of drug bound hyaluronan conjugates in cancer cells, we selected the MDA-1986 cells and an HA-Pt nanoconjugate as a model cell line and HA-drug conjugate. The results suggested that the HA-Pt conjugate is likely to be internalized via CD44-mediated endocytosis, and is not impacted by the blockage of the RHAMM and the LYVE-1 internalization pathways.

The uptake of platinum by cisplatin-treated cells was 60% greater than HA-Pt treated cells at 6 hours. This is consistent with the expected *in vitro* behavior of cisplatin. Cisplatin remains in the cell-permeable neutral form within the high-sodium cell culture media, until it diffuses into cells where it is hydrolyzed and trapped. Thus, cisplatin rapidly concentrates within cells *in vitro*. However, complexing cisplatin with HA maintains a large depot outside the cells since the HA complexes are not entirely internalized within this timeframe. *In vivo*, cisplatin cannot be safely injected into tissues because of its vessicating properties (Dernell et al., 1997, Bairey et al., 1997), and rapid clearance from the injection site by the diffusion into the vascular system would lead to minimum local anti-cancer benefit.

In contrast, the platinum concentrations in cisplatin-treated cells were independent of antibody exposure at all timepoints (Figure 9, t=1 and 24 h not shown), which is not unexpected as no studies in the literature have suggested the involvement of CD44, RHAMM or LYVE-1 receptors in the internalization of free cisplatin.

### 3.5 Platinum Concentrations in Tumor Xenografts

To compare the intratumoral platinum concentrations between cisplatin i.v. and HA-Pt s.c. therapies, HNSCC xenografts were excised and the platinum concentrations were determined using ICP-MS. The normalized intratumoralplatinum concentrations of s.c. HA-Pt treated animals were 7.7-, 8.3-, and 5.3-fold greater than the i.v. cisplatin treated animals, at 2, 24 and 48 hours post injection (Figure 10), respectively, which indicates that the bioavailability of the subcutaneously administered HA-Pt polymer drug conjugate is superior to the cisplatin i.v. therapy.

The MDA-1986 cells overexpress CD44, therefore the uptake of HA-Pt conjugates into the HNSCC xenografts may be regulated by a CD44-mediated mechanism. The finding that was reported in Figure 10 was consistent with our previous canine study, in which tumor-bearing dogs were treated with i.v. cisplatin or peritumoral HA-Pt. The HA-Pt treated dogs demonstrated significantly increased intratumoral concentrations of platinum compared to the i.v. cisplatin treated animals (Venable et al., 2012). However, the mice were injected peritumorally so mechanical deposition did not play a role in the increased tumor uptake. The locally injected HA-Pt conjugates could act as a sustained drug releasing depot, slowly generating platinum and delivering the drug into cancer cells via lymphatic vessels surrounding the tumor. There could also be a “neighbor effect” whereby cisplatin is released from dying cells into nearby tumor cells. HNSCC cells are known to express high levels of CD44 receptors (Joshua et al., 2012), thus the aforementioned differentiation between cisplatin and HA-Pt could be attributed to the receptor mediated active transport of the polymer drug conjugate via the major hyaluronan receptor, CD44.

## 4. Discussion

Many potent anti-cancer drugs that succeed *in vitro* fail to be efficacious*in vivo*, partially due to poor accumulation in the vicinity of the tumor mass and inadequate penetration into the tumor cells. This is especially true for intravenously infused chemotherapeutics that rely on passive diffusion to gain access to tumor cells. Localized drug delivery strategies, such as subcutaneous injection of drug encapsulated micelles or drug conjugated polymeric nanoparticles, help to overcome these obstacles by bypassing the vascular journey of an anticancer agent and directly administering the agent or carrier to the tumor and intended tissues.

Once drug carriers reach the immediate extracellular environment of the cancer cells from either the nearby injection site, if the drug is given locally, or from the blood capillaries, due to enhanced permeation and retention effect if the drug is given intravenously, carried-associated anti-cancer drugs enter cells via one or both of the following mechanisms. The carriers may release the drug in the tumor extracellular fluid, which has been shown to have a slightly more acidic pH of 6.5 to 7.2 compared to normal tissues; subsequently, drug molecules traverse cell membrane and reach the cytosol and eventually enter the nucleus. This mechanism applies to many drug carrier conjugates that are constructed using synthetic polymers, such as the HPMA-based cisplatin and oxaliplatin conjugates that have undergone phase 1 and 2 clinical trials (Rademaker-Lakhai et al., 2004). Unlike HA, there are no specific receptors known to date to naturally uptake synthetic polymers, such as HPMA,

PEGs and dendrimers. Although the HPMA-oxaliplatin conjugate AP5280 reported a much greater MTD, compared to the cisplatin or the carboplatin in the Phase I clinical trial, it is partially attributed to the fact that the majority of the drug may not get into cells. Leukocytes from patients who were given the AP5280 infusion had a smaller amount of detectable DNA-Pt adducts compared to patients who received intravenous cisplatin, despite AP5280 being dosed at a much higher level compared to the cisplatin. Drug delivery platforms that rely on passive cellular entry of the carrier or released drug molecules may not achieve sufficient levels of active drug in the cells, in addition, the drug or carrier could also traverse normal cells via passive diffusion leading to unwanted off-target toxicity.

Alternatively, carriers made of natural polymers or endogenous ligands, such as the hyaluronan conjugates reported here, may be internalized via receptor mediated endocytosis. In this case, the drug conjugated HA first binds to its primary cellular receptor, CD44, on the cell membrane, which then it is translocated into cells in a vesicular form. Subsequently, it fuses with acidic early endosomes, which have a pH of 6.0–6.5. Drug release into the cytosol may be triggered if the carrier system possesses a pH-sensitive or "tunable" drug release mechanism. Many drug-encapsulated, pH-sensitive micellar and liposomal drug delivery platforms take advantage of the pH-tunable release properties to deliver chemotherapeutics into cancer cells (Zhao et al., 2010, Chang et al., 2010, Yuba et al., 2014). In the next step of the endocytic pathway, drug-containing organelles may be further sorted into more acidic late endosomes (pH 5.0–6.0). Although there is a likelihood that the internalized drug molecules may be recycled back by the recycling endosomes, the drugs that escape the endosomes may successfully enter the cytosol or targeted organelles (e.g. nucleus or mitochondria) and trigger cell death. Our data suggests that these HA-based drug carriers utilize this internalization mechanism to enter cells, taking advantage of the overexpressed HA receptor CD44 on the cellular membrane of many cancer cells. Thus, it spares normal cells that do not overexpress the receptor from the harmful cytotoxin. In addition, highly metastatic cancer cell subpopulations have been shown to greatly overexpress CD44 receptor (Yae et al., 2012).

Based on our previous studies of the HA-DOX and the HA-Pt in rodents and canines, we believe that HA-based chemotherapeutics may work similarly to antibody-drug conjugates and polymer-antibody-drug conjugates in terms of targeting specificity. In addition, HA platforms utilize a natural polymer with a tropism to a receptor (CD44) overexpressed in many cancers, and thus these carriers do not require separate targeting with an antibody or peptide, which may translate into a lower cost of the treatment and a more stable formulation compared to the antibody-drug conjugates.

## 5. Conclusion

CD44-mediated uptake appears to be the predominant pathway for HA internalization in HNSCC cells. Other receptors, including RHAMM and LYVE-1, are not involved in nanoconjugate uptake in HNSCC cells. The conjugation of anti-cancer drugs, including cisplatin and doxorubicin, did not reduce the CD44 specificity of the uptake. The hyaluronan-conjugate drug delivery platform greatly enhanced intratumoral drug area-under-the-curve compared to conventional intravenous chemotherapy, which may translate

into improved anti-cancer efficacy *in vivo*. Furthermore, increased intra-tumoral drug accumulation may allow reduced total chemotherapy dosage and decreased dosing frequency, reducing their potential dose-limiting toxicities.

## Acknowledgements

The authors thank Drs. Jeff Krise and Randall Logan (University of Kansas) for their generous assistance in fluorescence microscopy studies. Dr. SuzellSiller (University of Kansas Medical Center) is thanked for assistance developing the animal tumor model.

This work was supported by awards from the American Cancer Society (RSG-08-133-01-CDD, Forrest), the NIH (R01-CA173292, Forrest), and the KINBRE. In addition, AA was supported by a fellowship from the King Saud University and the Saudi Arabia Government. WCM Forrest and Drs. ML Forrest, Cai and Shynader have financial interest in a company that has licensed technology for drug formulation with hyaluronan.

## References

Bairey O, Bishara J, Stahl B, Shaklai M. Severe tissue necrosis after cisplatin extravasation at low concentration: possible "immediate recall phenomenon". J Natl Cancer Inst. 1997; 89:1233–1234. [PubMed: 9274921]

Cai S, Thati S, Bagby TR, Diab HM, Davies NM, Cohen MS, Forrest ML. Localized doxorubicin chemotherapy with a biopolymeric nanocarrier improves survival and reduces toxicity in xenografts of human breast cancer. J Control Release. 2010a; 146:212–218. [PubMed: 20403395]

Cai S, Xie Y, Bagby TR, Cohen MS, Forrest ML. Intralymphatic chemotherapy using a hyaluronan-cisplatin conjugate. J Surg Res. 2008; 147:247–252. [PubMed: 18498877]

Cai S, Xie Y, Davies NM, Cohen MS, Forrest ML. Carrier-based intralymphatic cisplatin chemotherapy for the treatment of metastatic squamous cell carcinoma of the head & neck. Ther Deliv. 2010b; 1:237–245. [PubMed: 21339844]

Cai S, Xie Y, Davies NM, Cohen MS, Forrest ML. Pharmacokinetics and disposition of a localized lymphatic polymeric hyaluronan conjugate of cisplatin in rodents. J Pharm Sci. 2010c; 99:2664–2671. [PubMed: 19960530]

Chang C, Wang P, Yang H, Li L, Zhang LB. Expression of LYVE-1 and Prox-1 in non-small cell lung cancer and the relationship with lymph node metastasis. Sichuan Da Xue Xue Bao Yi Xue Ban. 2011; 42:174–178. [PubMed: 21500548]

Chang G, Li C, Lu W, Ding J. N-Boc-histidine-capped PLGA-PEG-PLGA as a smart polymer for drug delivery sensitive to tumor extracellular pH. Macromol Biosci. 2010; 10:1248–1256. [PubMed: 20593367]

Cohen MS, Cai S, Xie Y, Forrest ML. A novel intralymphatic nanocarrier delivery system for cisplatin therapy in breast cancer with improved tumor efficacy and lower systemic toxicity in vivo. Am J Surg. 2009; 198:781–786. [PubMed: 19969129]

Dernell WS, Withrow SJ, Straw RC, Lafferty MH. Adjuvant chemotherapy using cisplatin by subcutaneous administration. In Vivo. 1997; 11:345–350. [PubMed: 9292302]

Duvvuri M, Gong Y, Chatterji D, Krise JP. Weak base permeability characteristics influence the intracellular sequestration site in the multidrug-resistant human leukemic cell line HL-60. J Biol Chem. 2004; 279:32367–32372. [PubMed: 15181006]

Fraser JR, Laurent TC, Laurent UB. Hyaluronan: its nature, distribution, functions and turnover. J Intern Med. 1997; 242:27–33. [PubMed: 9260563]

Hall CL, Collis LA, Bo AJ, Lange L, Mcnicol A, Gerrard JM, Turley EA. Fibroblasts require protein kinase C activation to respond to hyaluronan with increased locomotion. Matrix Biol. 2001; 20:183–192. [PubMed: 11420150]

Johnson LA, Prevo R, Clasper S, Jackson DG. Inflammation-induced uptake and degradation of the lymphatic endothelial hyaluronan receptor LYVE-1. J Biol Chem. 2007; 282:33671–33680. [PubMed: 17884820]

Joshua B, Kaplan MJ, Doweck I, Pai R, Weissman IL, Prince ME, Ailles LE. Frequency of cells expressing CD44, a head and neck cancer stem cell marker: correlation with tumor aggressiveness. Head Neck. 2012; 34:42–49. [PubMed: 21322081]

Lunov O, Syrovets T, Rocker C, Tron K, Nienhaus GU, Rasche V, Mailander V, Landfester K, Simmet T. Lysosomal degradation of the carboxydextran shell of coated superparamagnetic iron oxide nanoparticles and the fate of professional phagocytes. Biomaterials. 2010; 31:9015–9022. [PubMed: 20739059]

Majumdar S, Tejo BA, Badawi AH, Moore D, Krise JP, Siahaan TJ. Effect of modification of the physicochemical properties of ICAM-1-derived peptides on internalization and intracellular distribution in the human leukemic cell line HL-60. Mol Pharm. 2009; 6:396–406. [PubMed: 19296614]

Malugin A, Kopeckova P, Kopecek J. Liberation of doxorubicin from HPMA copolymer conjugate is essential for the induction of cell cycle arrest and nuclear fragmentation in ovarian carcinoma cells. J Control Release. 2007; 124:6–10. [PubMed: 17869367]

Mouta Carreira C, Nasser SM, Di Tomaso E, Padera TP, Boucher Y, Tomarev SI, Jain RK. LYVE-1 is not restricted to the lymph vessels: expression in normal liver blood sinusoids and down-regulation in human liver cancer and cirrhosis. Cancer Res. 2001; 61:8079–8084. [PubMed: 11719431]

Rademaker-Lakhai JM, Terret C, Howell SB, Baud CM, De Boer RF, Pluim D, Beijnen JH, Schellens JH, Droz JP. A Phase I and pharmacological study of the platinum polymer AP5280 given as an intravenous infusion once every 3 weeks in patients with solid tumors. Clin Cancer Res. 2004; 10:3386–3395. [PubMed: 15161693]

Sakai-Kato K, Ishikura K, Oshima Y, Tada M, Suzuki T, Ishii-Watabe A, Yamaguchi T, Nishiyama N, Kataoka K, Kawanishi T, Okuda H. Evaluation of intracellular trafficking and clearance from HeLa cells of doxorubicin-bound block copolymers. Int J Pharm. 2012; 423:401–409. [PubMed: 22207161]

Shigeishi H, Fujimoto S, Hiraoka M, Ono S, Taki M, Ohta K, Higashikawa K, Kamata N. Overexpression of the receptor for hyaluronan-mediated motility, correlates with expression of microtubule-associated protein in human oral squamous cell carcinomas. Int J Oncol. 2009; 34:1565–1571. [PubMed: 19424574]

Singh M, Atwal H, Micetich R. Transferrin directed delivery of adriamycin to human cells. Anticancer Res. 1998; 18:1423–1427. [PubMed: 9673350]

Venable R, Worley D, Gustafson D, Hansen R, Ehrhart E, Cai S, Cohen M, Forrest L. Hyaluronan cisplatin conjugate in five dogs with soft tissue sarcomas. Am. J. Vet. Res. 2012 In Press.

Xie Y, Aillon KL, Cai S, Christian JM, Davies NM, Berkland CJ, Forrest ML. Pulmonary delivery of cisplatin-hyaluronan conjugates via endotracheal instillation for the treatment of lung cancer. Int J Pharm. 2010; 392:156–163. [PubMed: 20363303]

Yae T, Tsuchihashi K, Ishimoto T, Motohara T, Yoshikawa M, Yoshida GJ, Wada T, Masuko T, Mogushi K, Tanaka H, Osawa T, Kanki Y, Minami T, Aburatani H, Ohmura M, Kubo A, Suematsu M, Takahashi K, Saya H, Nagano O. Alternative splicing of CD44 mRNA by ESRP1 enhances lung colonization of metastatic cancer cell. Nat Commun. 2012; 3:883. [PubMed: 22673910]

Yamano Y, Uzawa K, Shinozuka K, Fushimi K, Ishigami T, Nomura H, Ogawara K, Shiiba M, Yokoe H, Tanzawa H. Hyaluronan-mediated motility: a target in oral squamous cell carcinoma. Int J Oncol. 2008; 32:1001–1009. [PubMed: 18425326]

Yuba E, Tajima N, Yoshizaki Y, Harada A, Hayashi H, Kono K. Dextran derivative-based pH-sensitive liposomes for cancer immunotherapy. Biomaterials. 2014; 35:3091–3101. [PubMed: 24406217]

Yue C, Liu P, Zheng M, Zhao P, Wang Y, Ma Y, Cai L. IR-780 dye loaded tumor targeting theranostic nanoparticles for NIR imaging and photothermal therapy. Biomaterials. 2013; 34:6853–6861. [PubMed: 23777910]

Zhao H, Duong HH, Yung LY. Folate-Conjugated Polymer Micelles with pH-Triggered Drug Release Properties. Macromol Rapid Commun. 2010; 31:1163–1169. [PubMed: 21590870]

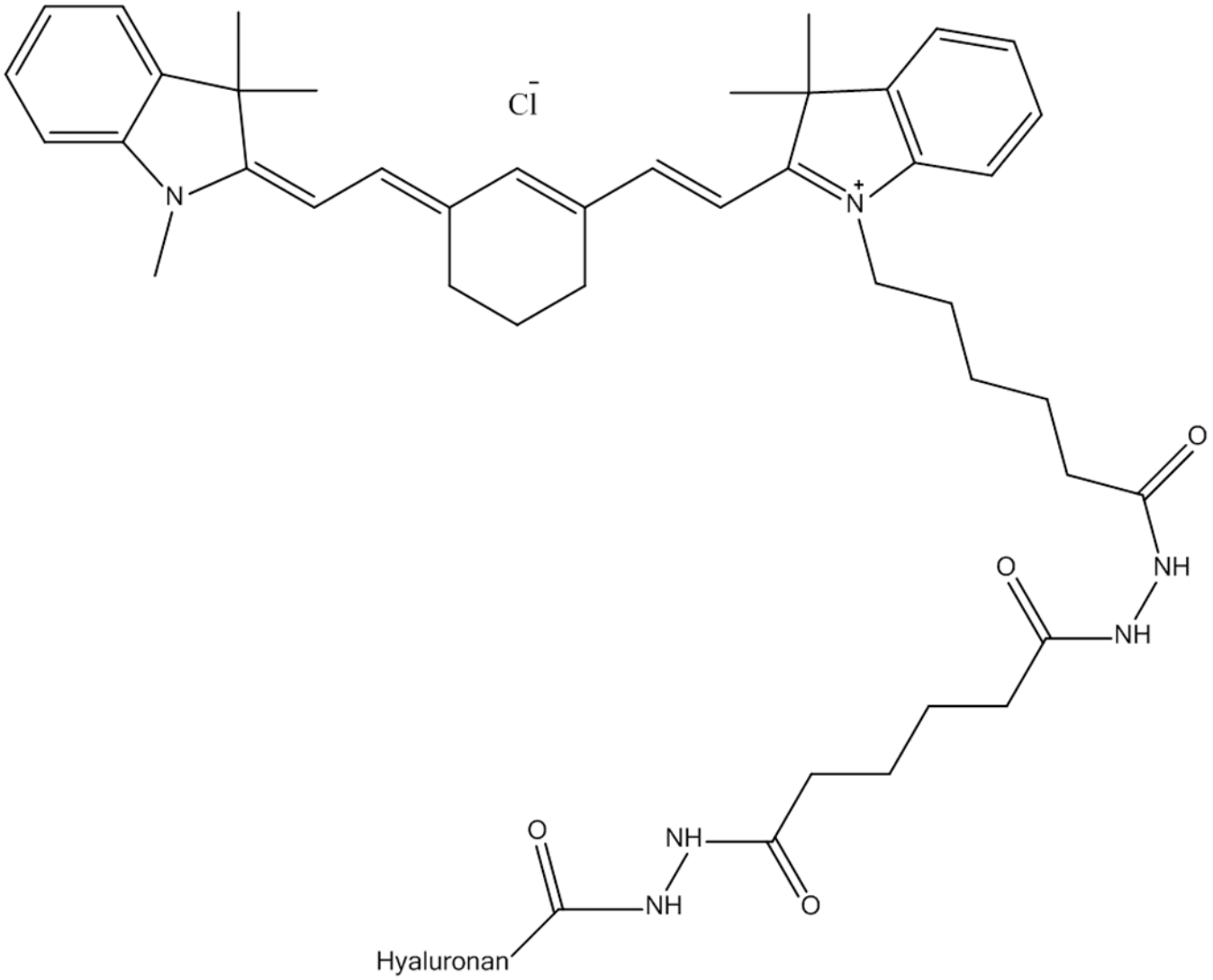


**Figure 1.**
Chemical structure of HA-Cy7.

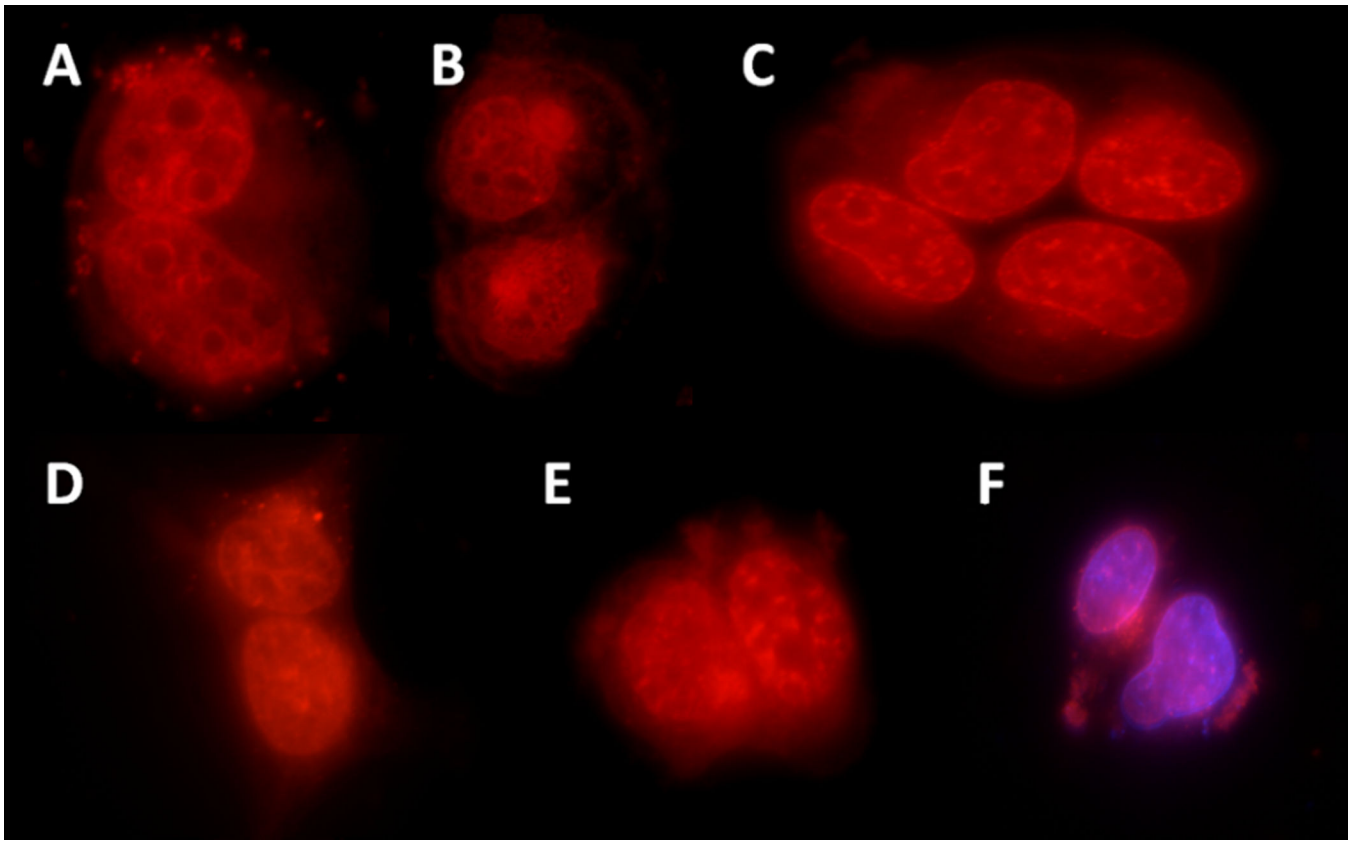


**Figure 2.**
Images of DOX (red) treated cells at: A) 15 m, B) 1h, C) 6 h, D) 24 h, E) 48 h, and F) 6 h co-stained with DAPI (purple).

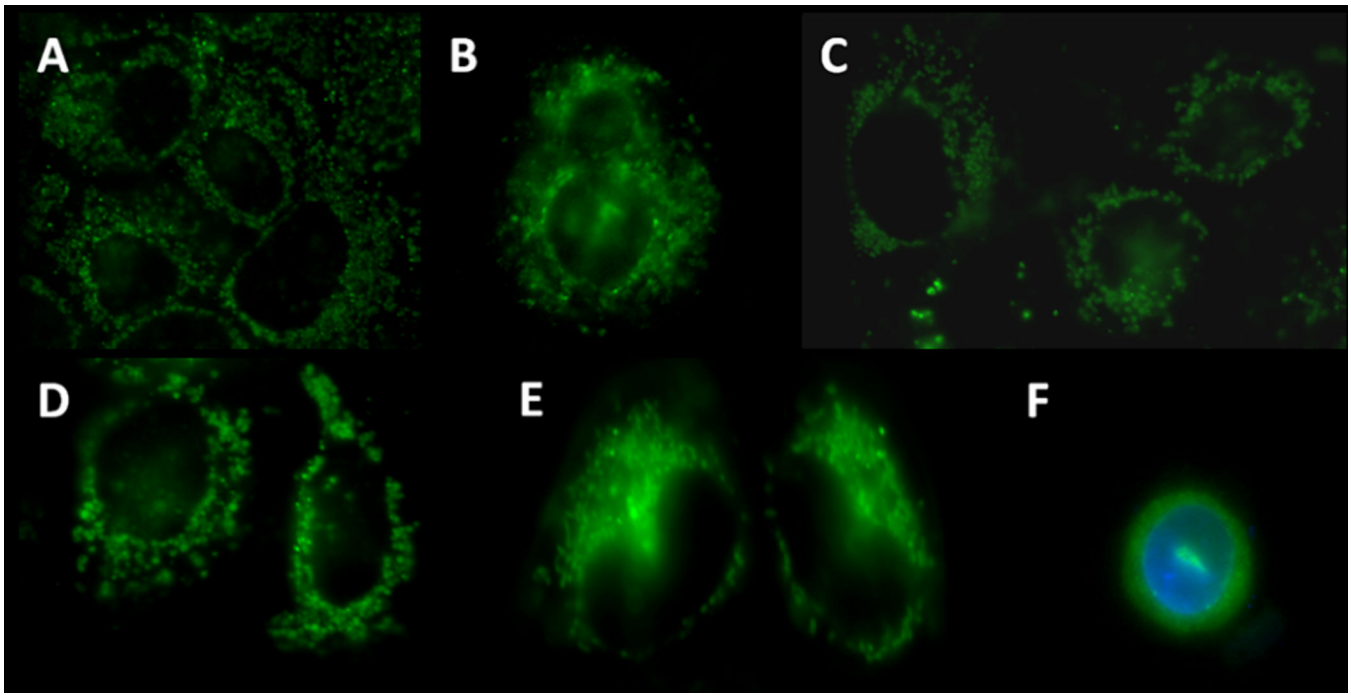


**Figure 3.**
Images of HA-Cy7 (green) treated cells at: A) 15 m, B) 1h, C) 6 h, D) 24 h, E) 48 h, and F) 6 h co-stained with DAPI (Blue).

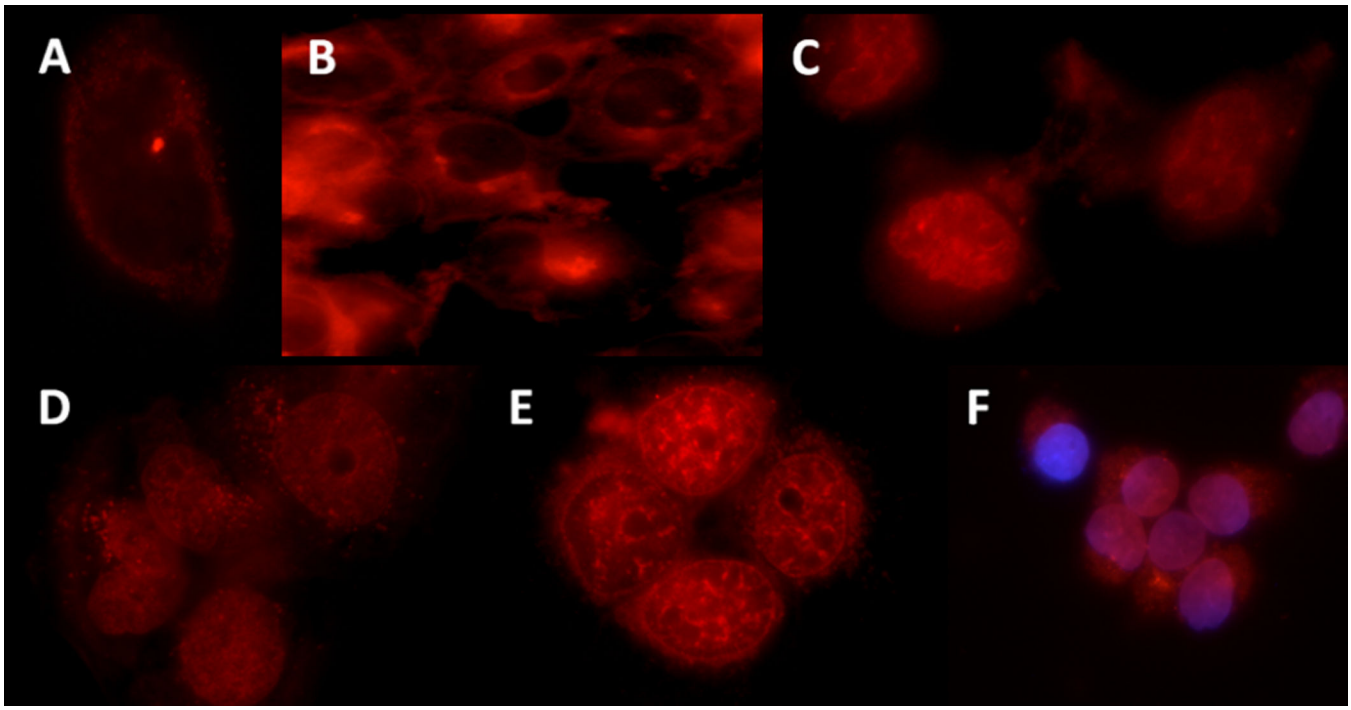


**Figure 4.**
Images of HA-DOX (red) treated cells at: A) 15 m, B) 1h, C) 6 h, D) 24 h, E) 48 h, and F) 6 h co-stained with DAPI (purple).

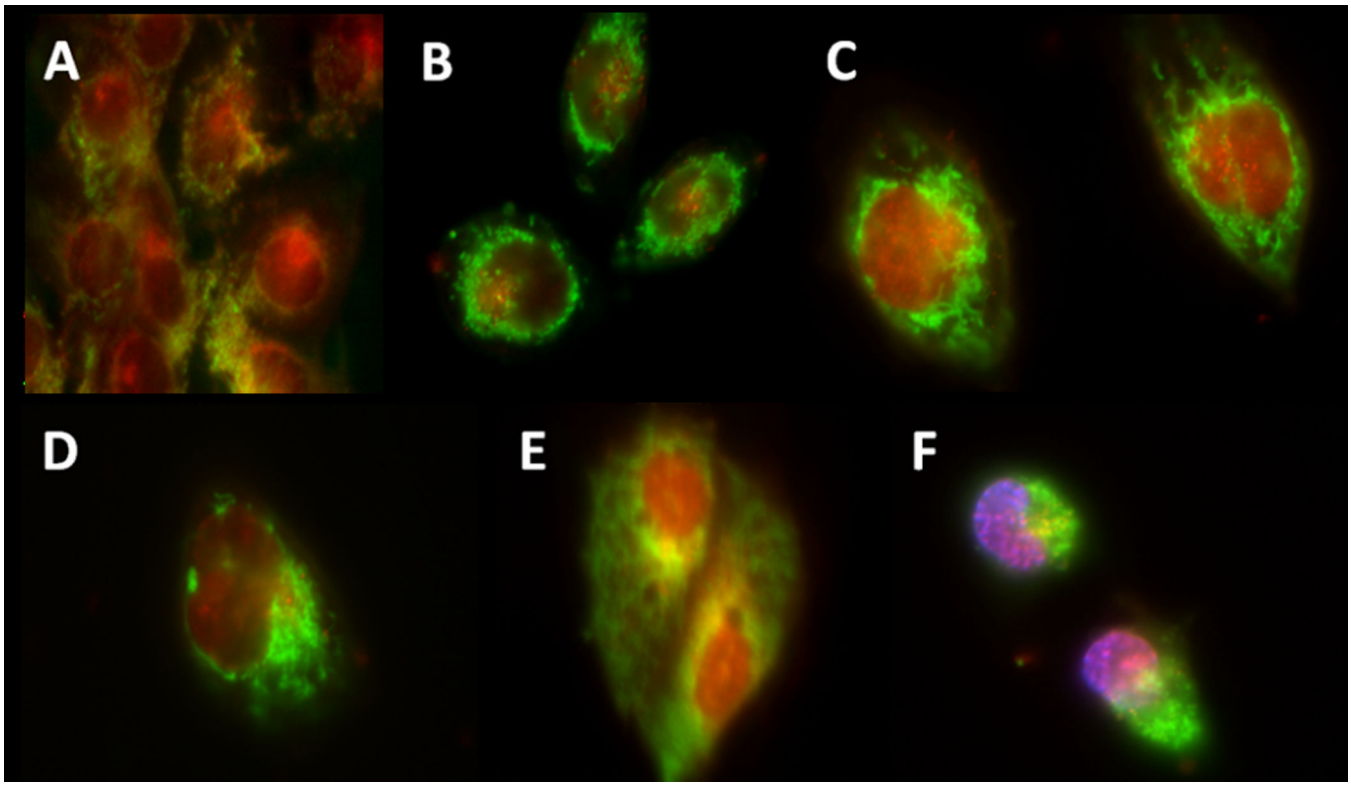


**Figure 5.**
Images of HA-DOX-Cy7 (DOX: red; Cy7: green) treated cells at: A) 15 m, B) 1h, C) 6 h, D) 24 h, E) 48 h, and F) 6 h co-stained with DAPI (purple).

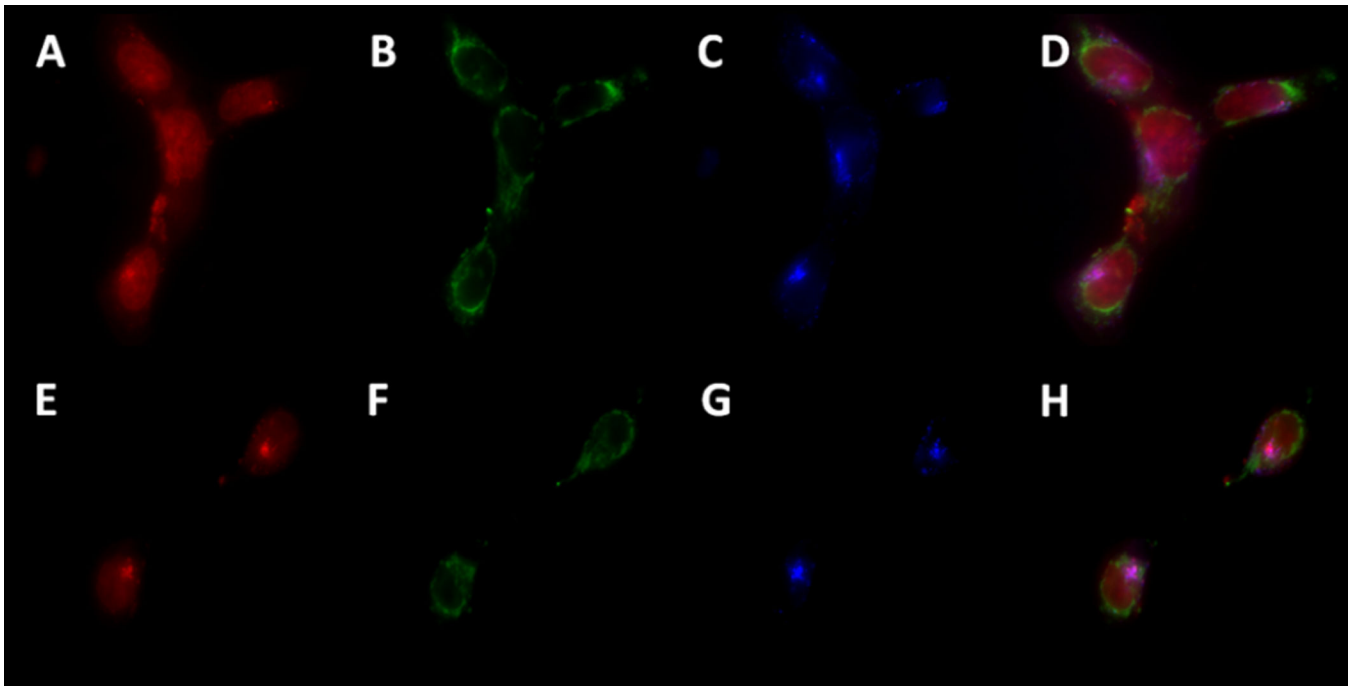


**Figure 6.**

Images of HA-DOX-Cy7 treated cells, co-stained using a lysotracker dye: A) and E) DOX (red), B) and F) Cy7 (green), C) and G) Lysotracker dye (blue), and D) and H) lysosomal DOX (purple).

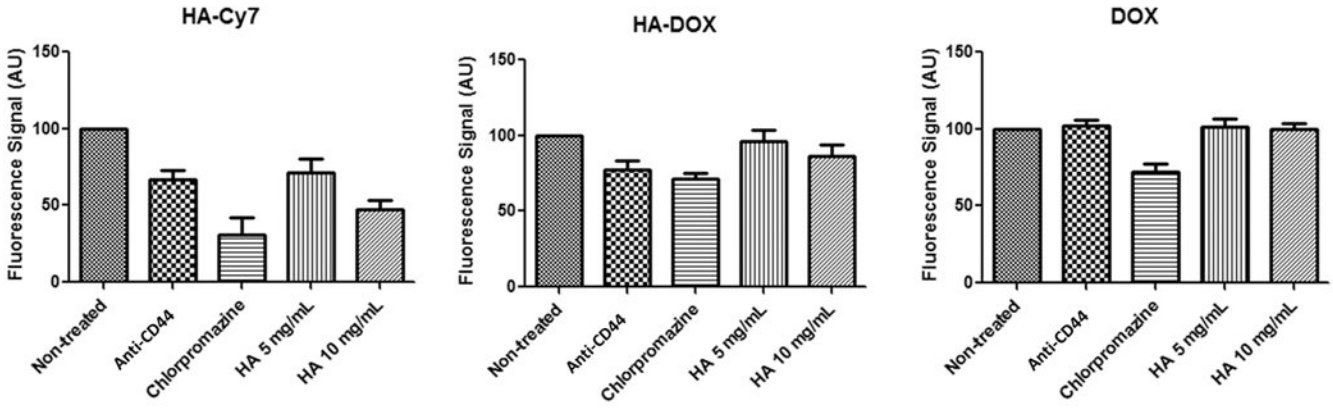


**Figure 7.**

The relative fluorescence intensity of HA–Cy7, HA-DOX and DOX treated cells. MDA-1986 cells were pretreated with 10–μg/ml anti-CD44 antibody (30 min), 25–μM chlorpromazine (30 min), 5–mg/ml HA (24 h), or 10–mg/ml HA (24 h).

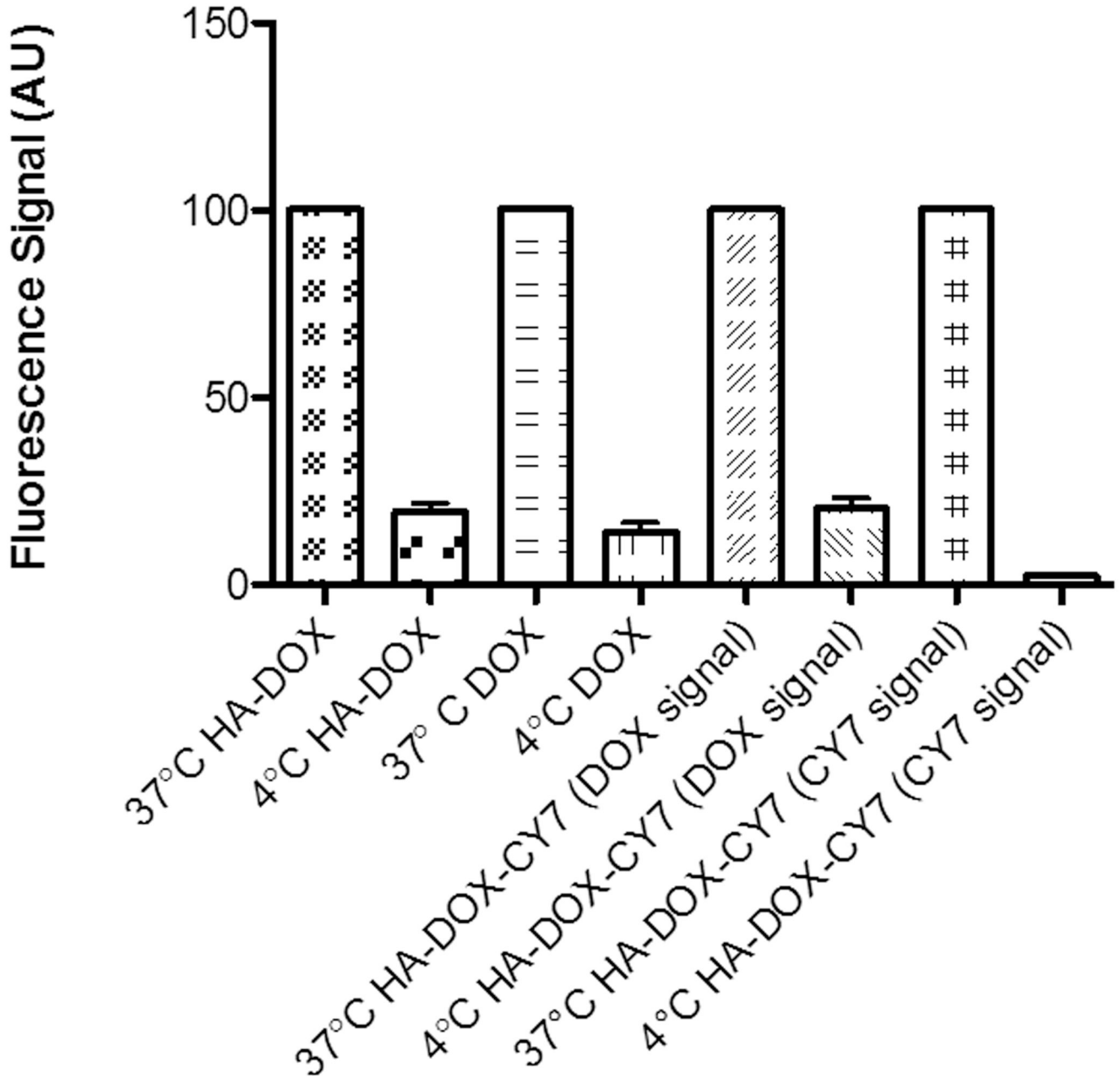


**Figure 8.**
Cellular fluorescence intensity after one hour incubation with HA-DOX, DOX and HA-DOX-Cy7 at 37°C and 4°C.

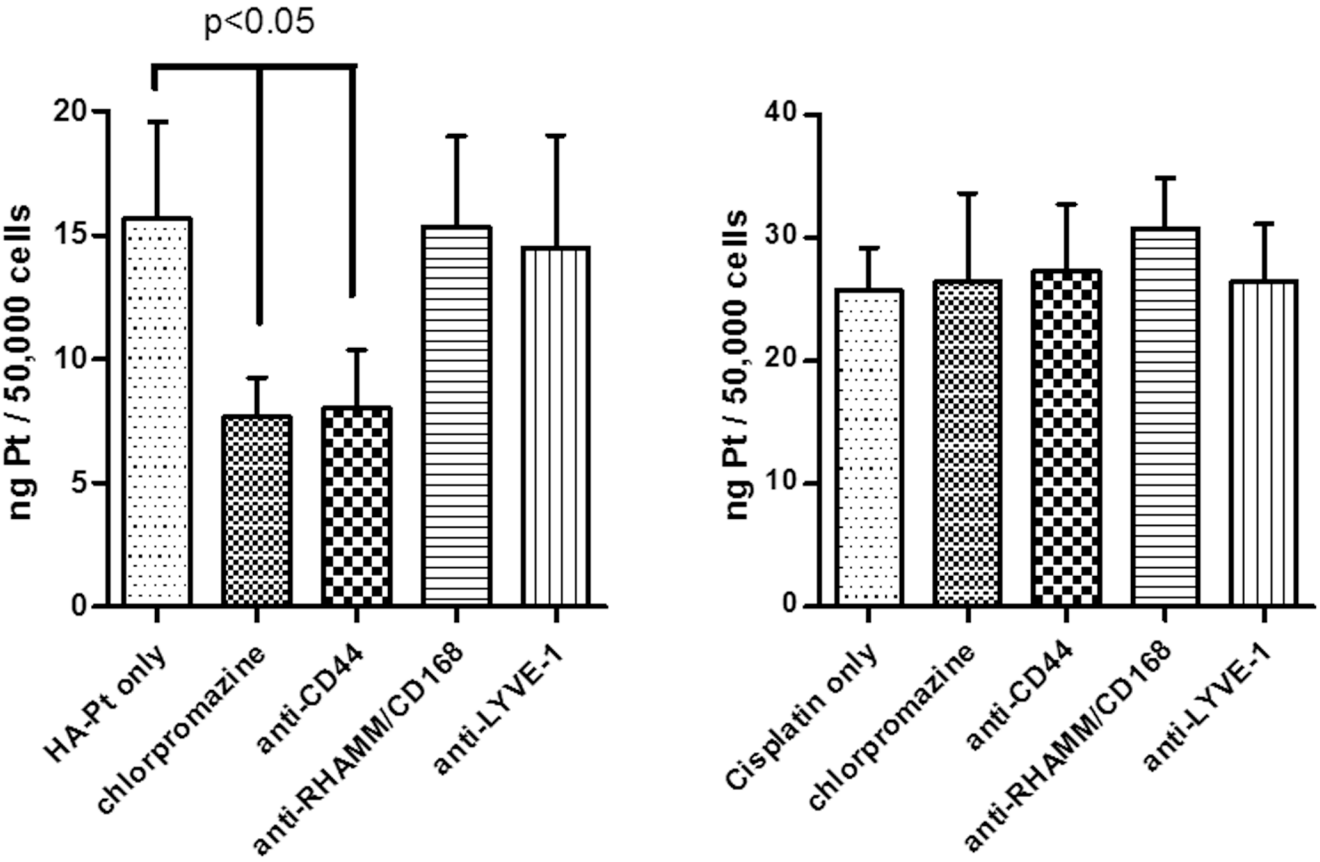


**Figure 9.**

Platinum concentrations in MDA-1986 cells. Cells were pretreated with 25-μM chlorpromazine, 10-μg/ml anti-CD44, anti-RHAMM, or anti-LYVE-1 antibodies for 1 h before the addition of 30-μg/ml HA-Pt (on platinum basis) and subsequent incubation for 6 h (HA-Pt only vs. anti-CD44: p=0.0154; HA-Pt only vs. chlorpromazine: p=0.0091). Nanoconjugate uptake was decreased significantly with CD44 antibody treatment and inhibition of clatherin-dependent endocytosis with chlorpromazine. CD44 and splice variant overexpression is associated with human cancers; blockage of less tumor-specific receptors of HA (e.g. LYVE-1 and RHAMM) did not significantly alter HA uptake in cancer cells. Free cisplatin controls (right panel) were not affected by antibody blocking (MDA-1986 cells were incubated with antibodies for 24 hrs and then exposed to nanoconjugates for 6 hrs before ICP-MS of the lysate). This suggested that drug conjugation did not alter CD44 specificity of HA.

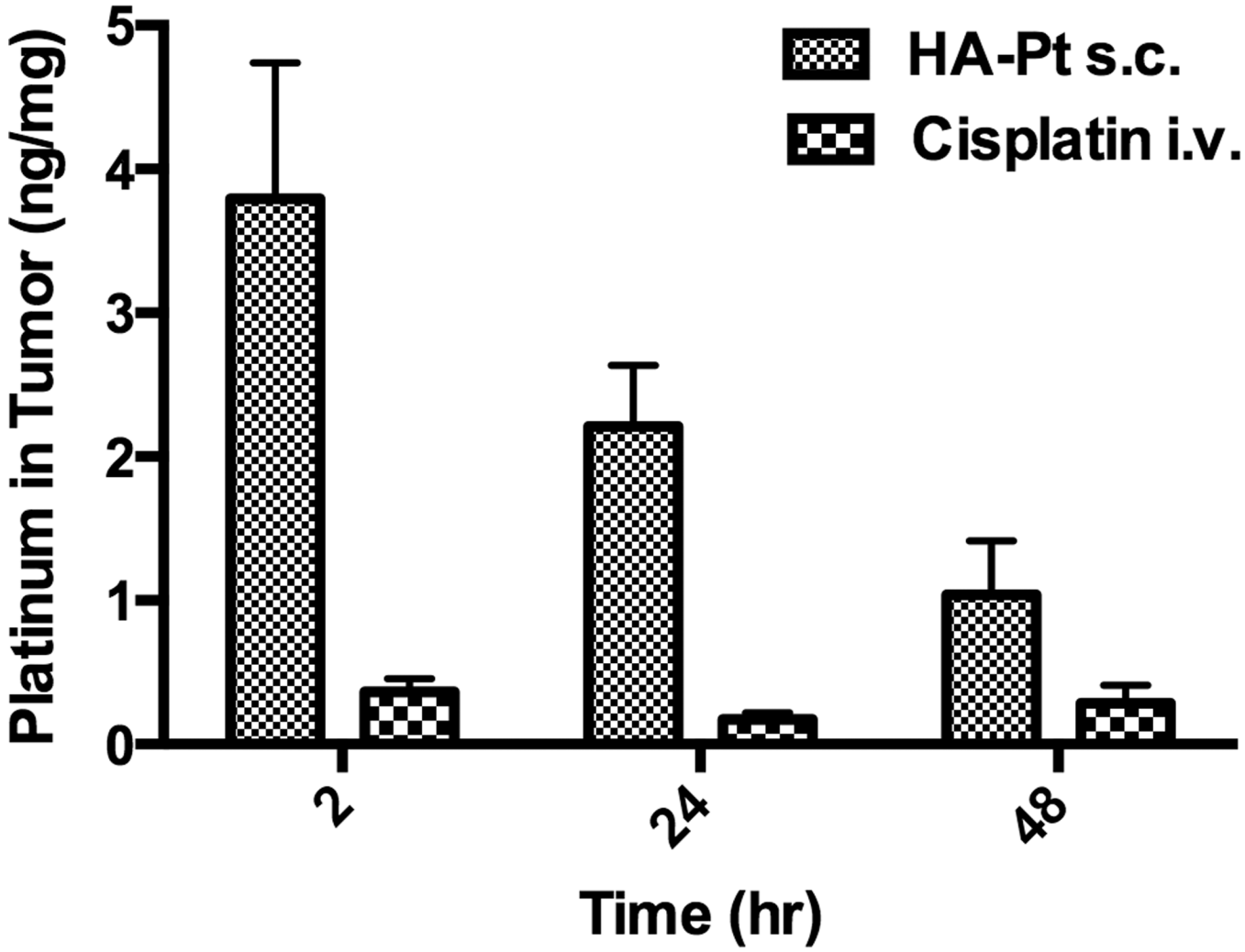


**Figure 10.**

Platinum concentrations in HNSCC xenografts. Mice were injected with MDA-1986 cells and treated with either i.v. cisplatin or s.c. HA-Pt at 5 mg/kg. Tumors were excised 2-, 24-, or 48-hours post injection (N=4/timepoint).